

Activation of Coordinated Carbon Dioxide in $\text{Fe}(\text{CO}_2)(\text{depe})_2$ by Group 14 Electrophiles

Masafumi Hirano, Masatoshi Akita, Kazuo Tani, Kuninori Kumagai, Noriko C. Kasuga,[†] Atsushi Fukuoka, and Sanshiro Komiya^{*,‡}

Department of Applied Chemistry, Faculty of Technology, Tokyo University of Agriculture and Technology, 2-24-16 Nakacho, Koganei, Tokyo 184, Japan

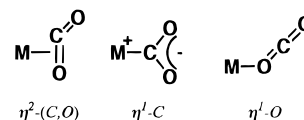
Received August 27, 1996[⊗]

A CO_2 complex of iron(0), $\text{Fe}(\text{CO}_2)(\text{depe})_2$ (**1**; depe = 1,2-bis(diethylphosphino)ethane) has been prepared by replacement of N_2 in $\text{Fe}(\text{N}_2)(\text{depe})_2$ by CO_2 . The X-ray structure analysis of **1** shows that it has a $\eta^2(\text{C}, \text{O})\text{-CO}_2$ ligand in a trigonal-bipyramidal Fe geometry with some contribution of an $\eta^1(\text{C})$ mode. Reaction of **1** with R_3SnCl in Et_2O at -78°C gives the iron carboxylate complexes $\text{FeCl}(\text{CO}_2\text{SnR}_3)(\text{depe})_2$ ($\text{R} = \text{Me}$, (**2a**), Ph (**2b**)). The X-ray structure analysis of **2b** shows that the CO_2 fragment bridges between the Fe and Sn atoms in a $\mu\text{-}\eta^1(\text{C}):\eta^2(\text{O}, \text{O})\text{-CO}_2$ fashion. Treatment of **1** with Me_3SiCl results in the removal of an O atom from the CO_2 ligand to give a cationic carbonyliron(II) complex, $[\text{FeCl}(\text{CO})(\text{depe})_2]^+\text{Cl}^-$ (**3a**), and $(\text{Me}_3\text{Si})_2\text{O}$. Similarly, **1** reacts with carbon electrophiles such as MeI and MeOTf to give the corresponding cationic iron(II) carbonyl complexes $[\text{FeX}(\text{CO})(\text{depe})_2]^+\text{X}^-$ ($\text{X} = \text{I}$ (**3b**), OTf (**3c**)) and Me_2O .

Introduction

The synthesis and chemical reactivities of transition-metal CO_2 complexes have attracted considerable attention toward the chemical fixation of CO_2 .¹ Formic acid, methyl formate, *N,N*-dimethylformamide, oxalic acid, methanol, and ethanol are catalytically obtained, and transition-metal CO_2 complexes or their derivatives are postulated as active key intermediates.¹ The mononuclear complexes having CO_2 ligand, can be roughly divided into three groups, according to their coordination mode (Chart 1). While the $\eta^2(\text{C}, \text{O})\text{-CO}_2$ ligand is formally considered to coordinate to a metal center via the π orbital of a $\text{C}=\text{O}$ bond, the $\eta^1(\text{C})\text{-CO}_2$ ligand binds to an electron-rich metal via the sp^2 orbital of the central carbon. Though $\eta^1(\text{O})\text{-CO}_2$ is also a possible coordination mode, this type of CO_2 complex can be observed only in matrices at low temperature and has never been isolated.² Among the CO_2 complexes reported to date, structurally characterized mononuclear

Chart 1



CO_2 complexes are still limited, since Aresta reported the first molecular structure of $\text{Ni}(\text{CO}_2)(\text{PCy}_3)_2$.³ For example, the CO_2 ligands in $\text{Ni}(\text{CO}_2)(\text{PCy}_3)_2$,³ $\text{Nb}(\text{C}_5\text{H}_4\text{-Me})_2(\text{CH}_2\text{SiMe}_3)(\text{CO}_2)$,⁴ $\text{Mo}(\text{CO}_2)_2(\text{CN}^i\text{Pr})(\text{PMe}_3)_3$,⁵ and $\text{Mo}(\text{CO}_2)_2(\text{CNCH}_2\text{Ph})(\text{PMe}_3)_3$ ⁵ display typical examples of the $\eta^2(\text{C}, \text{O})$ mode, and those in $\text{Ru}(\text{bpy})_2(\text{CO})(\text{CO}_2)$ ⁶ and $\text{RhCl}(\text{CO}_2)(\text{diars})_2$ ⁷ show the $\eta^1(\text{C})$ mode. Although the first CO_2 complex of iron(0), $\text{Fe}(\text{CO}_2)(\text{PMe}_3)_4$, was reported in 1977,⁸ no structural characterization of iron(0) CO_2 complexes has been performed. It has been predicted by a theoretical calculation on $\text{Fe}(\text{CO}_2)(\text{PH}_3)_4$ that the coordinated CO_2 ligand would have a character intermediate between the $\eta^2(\text{C}, \text{O})$ and $\eta^1(\text{C})$ modes.⁹ It is generally considered that the $\eta^1(\text{C})\text{-CO}_2$ ligand is susceptible to electrophilic attack on one of the oxygen atoms due to its high polarization. Although it is important to delineate the chemical properties of the coordinated CO_2 ligands in well-characterized complexes, such reports are still very limited to date.¹⁰ Herein we report the full description of the synthesis, the first molecular structure of a CO_2 complex of iron-

[†] Present address: Faculty of Science, Department of Material Science, Kanagawa University, Kanagawa, Japan.

[‡] E-mail: komiya@cc.tuat.ac.jp. Fax: +81-423-87-7500.

[⊗] Abstract published in *Advance ACS Abstracts*, August 15, 1997.

(1) Reviews: (a) Darensbourg, D. J.; Kudarsky, R. A. *Adv. Organomet. Chem.* **1983**, *22*, 129. (b) Walther, D. *Coord. Chem. Rev.* **1987**, *79*, 135. (c) Behr, A. *Angew. Chem., Int. Ed. Engl.* **1988**, *27*, 661. (d) Behr, A. *Carbon Dioxide Activation by Metal Complexes*; VCH: Weinheim, Germany, 1988. (e) Walther, D. In *Enzymatic and Model Carboxylation and Reductions for Carbon Dioxide Utilization*; Aresta, M., Schloss, J. V., Eds.; NATO ASI Series C314; Kluwer: Dordrecht, The Netherlands, 1990. (f) Burgemeister, T.; Kastner, F.; Leitner, W. *Angew. Chem., Int. Ed. Engl.* **1993**, *32*, 739. (g) Gassner, F.; Leitner, W. *J. Chem. Soc., Chem. Commun.* **1993**, 1465. (h) Leitner, W. *Angew. Chem., Int. Ed. Engl.* **1994**, *33*, 173. (i) Jessop, P. G.; Ikariya, T.; Noyori, R. *Nature* **1994**, *368*, 231. (j) Ikariya, T.; Jessop, P. G.; Tokunaga, M.; Noyori, R. *Yuuki Gousei Kagaku Kyokaiishi* **1994**, *52*, 1032. (k) Jessop, P. G.; Ikariya, T.; Noyori, R. *Science* **1995**, *269*, 1065. (l) Jessop, P. G.; Hsiao, Y.; Ikariya, T.; Noyori, R. *Chem. Rev.* **1995**, *95*, 259. (m) Jessop, P. G.; Hsiao, Y.; Ikariya, T.; Noyori, R. *J. Chem. Soc., Chem. Commun.* **1995**, 707. (n) Jessop, P. G.; Hsiao, Y.; Ikariya, T.; Noyori, R. *J. Am. Chem. Soc.* **1996**, *118*, 344.

(2) (a) Mascetti, J.; Tranquille, M. *J. Phys. Chem.* **1988**, *92*, 2177. (b) However, contribution of the $\eta^1(\text{O})\text{-CO}_2$ mode is proposed in the dynamic process of $\text{Ni}(\text{CO}_2)(\text{PCy}_3)_2$: Jegat, C.; Fouassier, M.; Tranquille, M.; Mascetti, J.; Tommasi, I.; Aresta, M.; Ingold, F.; Dedieu, A. *Inorg. Chem.* **1993**, *32*, 1279.

(3) Aresta, M.; Nobile, C. F.; Albano, V. G.; Forni, E.; Manassero, M. *J. Chem. Soc., Chem. Commun.* **1975**, 636.

(4) Bristow, G. S.; Hitchcock, P. B.; Lappert, M. F. *J. Chem. Soc., Chem. Commun.* **1981**, 1145.

(5) (a) Alvarez, R.; Carmona, E.; Marin, J. M.; Poveda, M. L.; Gutierrez-Puebla, E.; Monge, A. *J. Am. Chem. Soc.* **1986**, *108*, 2286. (b) Alvarez, R.; Carmona, E.; Marin, J. M.; Monge, A.; Gutierrez-Puebla, E.; Poveda, M. L. *J. Chem. Soc., Chem. Commun.* **1984**, 1326.

(6) Tanaka, H.; Nagano, H.; Peng, S.; Tanaka, K. *Organometallics* **1992**, *11*, 1450.

(7) Calabrese, J. C.; Herskovitz, T.; Kinney, J. B. *J. Am. Chem. Soc.* **1983**, *105*, 5914.

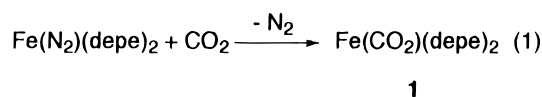
(8) Karasch, H. H. *Chem. Ber.* **1977**, *110*, 2213.

(9) (a) Jegat, C.; Fouassier, M.; Mascetti, J. *Inorg. Chem.* **1991**, *30*, 1521. (b) Jegat, C.; Fouassier, M.; Tranquille, M.; Mascetti, J. *Inorg. Chem.* **1991**, *30*, 1529.

(0), Fe(CO₂)(depe)₂ (**1**), and the chemical reactions of **1** with group 14 electrophiles resulting in C–O bond fission via iron carboxylate complexes. Part of these results has been published as a communication.¹¹

Results and Discussion

Preparation and Molecular Structure of Fe(CO₂)(depe)₂ (1**).** The CO₂ complex of iron(0) Fe(CO₂)(depe)₂ (**1**; depe = 1,2-bis(diethylphosphino)ethane) is synthesized by replacement of N₂ in Fe(N₂)(depe)₂¹² with a stoichiometric amount of CO₂ in THF at room temperature (eq 1).



The IR spectrum of **1** in a KBr disk shows sharp and characteristic $\nu(\text{C}=\text{O})$, $\nu(\text{C}-\text{O})$ and $\delta(\text{OCO})$ bands at 1630 (vs), 1096 (vs), and 730 (s) cm⁻¹, respectively, which are very similar to those of the analog Fe(CO₂)(PMe₃)₄ (1620, 1108, and 623 cm⁻¹).⁸ It is worthwhile to note that **1** exclusively gives a single set of $\nu(\text{C}=\text{O})$, $\nu(\text{C}-\text{O})$, and $\delta(\text{OCO})$ bands, which shows that the CO₂ ligand coordinates to the iron center in a single geometry. On the other hand, two sets of $\nu(\text{C}=\text{O})$ bands are observed for typical zerovalent $\eta^2(\text{C},\text{O})$ -CO₂ complexes such as Ni(CO₂)(PEt₃)₂,¹³ Ni(CO₂)(PⁿBu₃)₂,¹³ Pd(CO₂)(PMePh₂)₂,¹⁴ and *trans*-Mo(CO₂)₂(PMe₃)₄.¹⁵ Sakaki suggested that the CO₂ ligand in Fe(CO₂)(PH₃)₄ coordinates in an equatorial plane in a pseudo-trigonal-bipyramidal geometry and the perpendicular coordination of CO₂ is very unstable because of a weak interaction between $d\pi(\text{metal HOMO})$ and $p\pi^*(\text{CO}_2 \text{ LUMO})$ orbitals.¹⁶ Therefore, **1** would have a CO₂ ligand in its equatorial plane in the solid state. The splitting between these $\nu(\text{C}=\text{O})$ and $\nu(\text{C}-\text{O})$ bands is a good criterion for unequivocal characterization of the coordination mode of the CO₂ ligand, in which the splitting of the $\eta^1(\text{C})$ mode is smaller than 400 cm⁻¹, while that of the $\eta^2(\text{C},\text{O})$ mode is normally larger than 500 cm⁻¹.^{9b} The band splitting for **1** (524 cm⁻¹) indicates that complex **1** basically has a $\eta^2(\text{C},\text{O})$ -CO₂ ligand in the solid state. The $\nu(\text{C}=\text{O})$ band of **1** (1630 cm⁻¹) appears at relatively low frequency among zerovalent CO₂ complexes, which implies strong back-donation from the electron-rich iron(0)

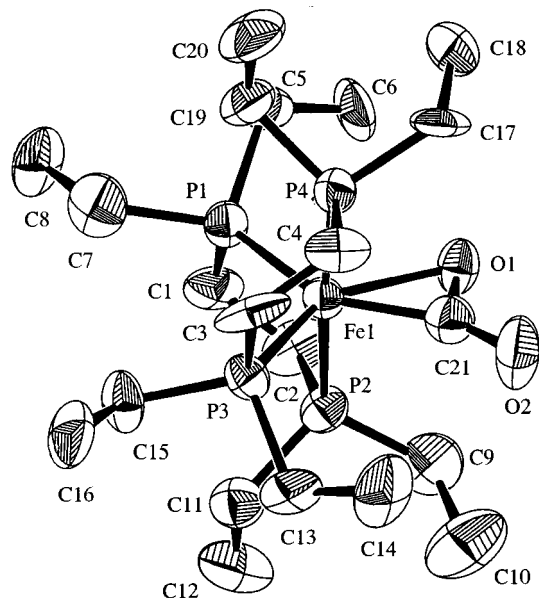


Figure 1. Molecular structure of Fe(CO₂)(depe)₂ (**1**).¹¹ Hydrogen atoms are omitted for clarity.

Table 1. Selected Bond Distances (Å) and Angles (deg) in Fe(CO₂)(depe)₂ (**1**)

Fe(1)–P(1)	2.271(6)	Fe(1)–P(2)	2.247(6)
Fe(1)–P(3)	2.192(6)	Fe(1)–P(4)	2.225(6)
Fe(1)–O(1)	2.08(1)	Fe(1)–C(21)	1.86(3)
O(1)–C(21)	1.28(2)	O(2)–C(21)	1.25(3)
P(1)–Fe(1)–P(2)	84.3(2)	P(1)–Fe(1)–P(3)	110.6(2)
P(1)–Fe(1)–P(4)	98.9(2)	P(2)–Fe(1)–P(3)	97.0(2)
P(2)–Fe(1)–P(4)	175.4(3)	P(2)–Fe(1)–O(1)	86.1(4)
P(2)–Fe(1)–C(21)	90.9(7)	P(3)–Fe(1)–P(4)	84.9(2)
P(4)–Fe(1)–O(1)	89.8(4)	P(4)–Fe(1)–C(21)	84.5(7)
O(1)–Fe(1)–C(21)	37.4(6)	O(1)–C(21)–O(2)	124(2)

center. An ABMX pattern is observed in the ³¹P{¹H} NMR spectrum of **1**, suggesting a trigonal-bipyramidal geometry. The ¹³C{¹H} NMR spectrum of **1** shows a quintet at 196.6 ppm, which is assignable to the coordinated CO₂ accidentally having the same coupling constant ($J = 38$ Hz) to the four phosphorus nuclei. The low molar electric conductivity of **1** ($\Lambda = 0.0168$ S cm² mol⁻¹) shows nonionic character in solution. The molecular structure of **1** is shown in Figure 1, and selected bond distances and angles are given in Table 1. Details of the crystal data have been published elsewhere.¹¹

Complex **1** has an essentially trigonal-bipyramidal geometry (P(1)–Fe–P(3) = 110.6(2)° and P(2)–Fe–P(4) = 175.4(3)°), where the coordinated CO₂ lies on the equatorial plane in the $\eta^2(\text{C},\text{O})$ mode. The bond distances of O(1)–C(21) (1.28(2) Å) and O(2)–C(21) (1.25(3) Å) are almost comparable to each other and are longer than that of free CO₂ (1.16 Å). It is worthwhile to note that the Fe(1)–C(21) bond distance (1.86(3) Å) is remarkably shorter than that of Fe–O(1) (2.08(1) Å) when the covalent bond diameters of the atoms are taken into account (sp² covalent radii: C, 0.67 Å, O, 0.62 Å).¹⁷ The O(1)–C(21)–O(2) angle of **1** (124(2)°) is relatively small and is close to that of the only $\eta^1(\text{C})$ mode ever reported (*cf* 121(1)° for Ru(bpy)₂(CO)($\eta^1(\text{C})$ -CO₂),⁶ and 126(2)° for RhCl($\eta^1(\text{C})$ -CO₂)(diars)₂).⁷ These facts indicate that the Fe atom in fact slides along the

(10) See for example: (a) Belmore, K. A.; Vanderpool, R. A.; Tsai, J.; Khan, M. A.; Nicholas, K. M. *J. Am. Chem. Soc.* **1988**, *110*, 2004. (b) Tsai, J.; Khan, M. A.; Nicholas, K. M. *Organometallics* **1989**, *8*, 2967; **1991**, *10*, 29. (c) Aresta, M.; Wuarana, E.; Tommasi, I. *J. Chem. Soc., Chem. Commun.* **1988**, 450. (d) Harlow, R. L.; Kinney, J. B.; Herskovitz, T. *J. Chem. Soc., Chem. Commun.* **1980**, 813. (e) Forschnew, T.; Menard, K.; Cutler, A. R. *J. Chem. Soc., Chem. Commun.* **1984**, 121. (f) Giuseppetti, M. E.; Cutler, A. R. *Organometallics* **1987**, *6*, 970. (g) Senn, D. R.; Gladysz, J. A.; Emerson, K.; Larsen, R. D. *Inorg. Chem.* **1977**, *11*, 2213.

(11) Komiya, S.; Akita, M.; Kasuga, N.; Hirano, M.; Fukuoka, A. *J. Chem. Soc., Chem. Commun.* **1994**, 1115. Full details of the crystal structure determination of **1** are given in the Supporting Information to that paper or may be obtained from the Cambridge Crystallographic Data Centre.

(12) Komiya, S.; Akita, M.; Yoza, A.; Kasuga, N.; Fukuoka, A.; Kai, Y. *J. Chem. Soc., Chem. Commun.* **1993**, 787.

(13) Aresta, M.; Nobile, C. F. *J. Chem. Soc., Dalton Trans.* **1977**, 708.

(14) Sakamoto, M.; Shimizu, I.; Yamamoto, A. *Organometallics* **1994**, *13*, 407.

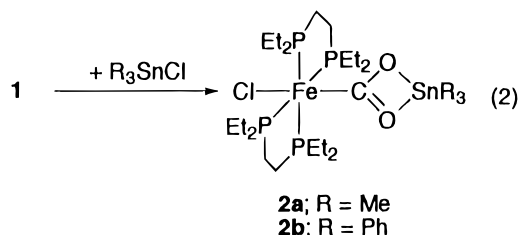
(15) Alvarez, R.; Carmona, E.; Marin, J. M.; Poveda, M. L.; Gutiérrez-Puebla, E.; Monge, A. *J. Am. Chem. Soc.* **1986**, *108*, 2286.

(16) Sakaki, S. *Stereochemistry of Organometallic and Inorganic Compounds*; Elsevier: Amsterdam, 1990.

(17) (a) Emsley, J. *The Elements*, 2nd ed.; Clarendon: Oxford, U.K., 1991. (b) Nippon Kagakukai. *Kagaku Binran II (The Handbook of Chemistry)*, 2nd ed.; Maruzen: Tokyo, 1975.

C–O linkage to the center carbon, implying considerable contribution of the $\eta^1(C)$ mode to the $\eta^2(C,O)$ -CO₂ ligand on iron(0). This result is consistent with the previously proposed structure for Fe(CO)₂(PMe₃).⁹ The contribution of the $\eta^1(C)$ mode may be due to the strong electron donation from Fe to CO₂, and it would make the oxygen atoms in the CO₂ ligand more susceptible to attack by electrophiles.

Reaction of 1 with Organotin Chlorides. To reveal the nucleophilicity of the coordinated CO₂ in **1**, reactions of **1** with organotin chlorides were carried out. Treatment of **1** with Me₃SnCl in Et₂O at –78 °C yields a new stannyl iron carboxylate complex FeCl(CO₂SnMe₃)(depe)₂ (**2a**), which can be recrystallized from Et₂O as reddish orange cubes (eq 2). Treatment of **1** with Ph₃SnCl gave an analogous stannyl ferracarboxylate complex FeCl(CO₂SnPh₃)(depe)₂ (**2b**).



The IR spectrum of **2a** shows a weak $\nu(C=O)$ band at 1338 cm⁻¹ assignable to $\mu\text{-}\eta^1(C)\text{:}\eta^2(O,O)\text{-CO}_2$ (1480–1312 cm⁻¹).^{18–20} The ¹H NMR spectrum of **2a** shows a singlet at 0.22 ppm with Sn satellites (²J_{Sn–H} = 71 Hz) due to the SnMe₃ group. Observations of a singlet at 71.6 ppm in the ³¹P{¹H} NMR spectrum and a quintet at 239.5 ppm (²J_{C–P} = 24 Hz) in the ¹³C{¹H} NMR spectrum assignable to the carboxylato carbon indicate the existence of the four magnetically equivalent phosphorus nuclei, implying that the DEPE ligands occupy the sites in the same equatorial plane of an octahedral geometry.

The X-ray structure analysis of **2b** established that it has a typical octahedral geometry where the CO₂ moiety bridges between the Fe and Sn atoms in a $\mu\text{-}\eta^1(C)\text{:}\eta^2(O,O)\text{-CO}_2$ mode. An ORTEP drawing of **2b** is given in Figure 2, and selected bond distances and angles are listed in Table 2.

The Fe(1)–C(21) bond distance in **2b** (1.87(1)°) is almost comparable to that in **1** (1.86(3)°). The O(1)–C(21) (1.32(1) Å) and O(2)–C(21) (1.28(1) Å) bond distances are not equal to each other. In addition, the Sn(1)–O(1) bond distance (2.097(6) Å) is substantially shorter than that of Sn(1)–O(2) (2.312(7) Å), and the internal angles among the O(1), C(21), O(2), and Sn(1) atoms add up to 360.1°. Thus, the atoms O(1), C(21), O(2), and Sn(1) constitute a distorted-trapezoidal plane. From these results, it can be considered that the Sn(1)–O(2) bond has more dative bond character, while the Sn(1)–O(1) bond has more covalent character. The overall structure of **2b** basically resembles that of other dinuclear metal carboxylates such as FeCp(CO₂SnPh₃)(CO)(PPh₃),¹⁸ FeCp*(CO₂SnR₃)(CO)₂,¹⁹ ReCp*(CO₂SnPh₃)(CO)(NO),²⁰ and ReCp(CO₂SnPh₃)(CO)(NO),²⁰

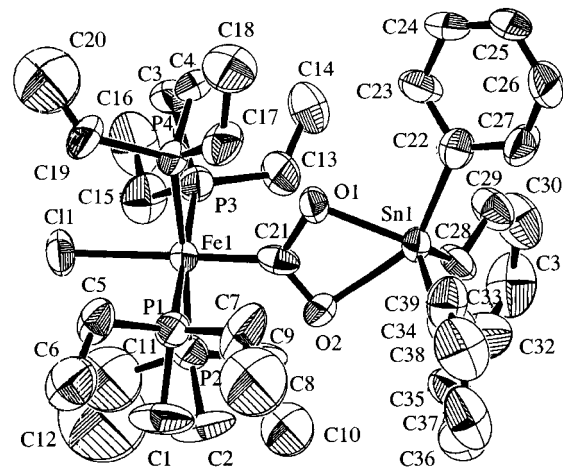


Figure 2. Molecular structure of FeCl(CO₂SnPh₃)(depe)₂ (**2b**). Hydrogen atoms are omitted for clarity.

Table 2. Selected Bond Distances (Å) and Angles (deg) in FeCl(CO₂SnPh₃)(depe)₂ (**2b**)

Fe(1)–C(21)	1.87(1)	Fe(1)–Cl(1)	2.398(3)
O(1)–C(21)	1.32(1)	O(2)–C(21)	1.28(1)
Sn(1)–O(1)	2.097(6)	Sn(1)–O(2)	2.312(7)
Sn(1)–C(22)	2.13(1)	Sn(1)–C(28)	2.11(1)
Sn(1)–C(34)	2.09(1)		
Cl(1)–Fe(1)–C(21)	179.0(3)	P(1)–Fe(1)–C(21)	89.5(3)
P(2)–Fe(1)–C(21)	89.5(3)	P(3)–Fe(1)–C(21)	90.4(3)
P(4)–Fe(1)–C(21)	93.1(3)	O(1)–C(21)–O(2)	108.4(9)
O(1)–Sn(1)–C(28)	113.0(3)	O(1)–Sn(1)–C(34)	117.1(3)
C(22)–Sn(1)–C(28)	108.8(4)	C(22)–Sn(1)–C(34)	104.9(3)
C(28)–Sn(1)–C(34)	117.3(4)	Sn(1)–O(1)–C(21)	101.8(6)
Sn(1)–O(2)–C(21)	92.9(6)		

which are prepared by the metathesis of metal carboxylates. However, the present transformation from a coordinated CO₂ to a metal carboxylate is unprecedented to our knowledge.^{21–28} In addition, it is noteworthy that most metal carboxylate complexes are stabilized by cyclopentadienyl or pentamethylcyclopentadienyl ligands and the stabilization of the present complex by phosphine ligands is relatively rare.

These complexes have relatively low field carboxylato resonances in the ¹³C{¹H} NMR spectra (**2a**, 239.5 ppm; **2b**: 243.8 ppm), which implies that they are not simple carboxylato groups in solution. Two canonical structures of the carboxylato moiety in $\mu\text{-}\eta^1(C)\text{:}\eta^2(O,O)$ metal

(21) By the metathesis reaction of iron(II) or rhenium(III) carboxylate with organotin chloride: (a) *Cf.* ref 18–20. (b) Gibson, D. H.; Ye, M.; Sleadd, B. A.; Mehta, J. M.; Mbadike, O. P.; Richardson, J. F.; Mashuta, M. S. *Organometallics* **1995**, *14*, 1242.

(22) By the reaction of metal carbonyls with tungsten oxide: Pilato, R. S.; Housmekerides, C. E.; Jernakoff, P.; Rubin, D.; Geoffroy, G. L.; Rheingold, A. L. *Organometallics* **1990**, *9*, 2333.

(23) By insertion of CO₂ in a metallocene–zirconocene complex: Pinkes, J. R.; Steffy, B. D.; Vites, J. C.; Cutler, A. R. *Organometallics* **1994**, *13*, 21.

(24) By dehydration of platinum carboxylate with platinum hydroxide: Bennett, M. A.; Robertson, G. B.; Rokicki, A.; Wickramasinghe, W. A. *J. Am. Chem. Soc.* **1988**, *110*, 7098.

(25) By deprotonation of rhenium carboxylate with transition-metal tetrafluoroborates: Gibson, D. H.; Franco, J. O.; Mehta, J. M.; Mashuta, M. S.; Richardson, J. F. *Organometallics* **1995**, *14*, 5068.

(26) By the intermolecular coupling reactions of ruthenium or rhenium carboxylates with zirconocene derivatives: Gibson, D. H.; Mehta, J. M.; Sleadd, B. A.; Mashuta, M. S.; Richardson, J. F. *Organometallics* **1995**, *14*, 4886.

(27) By ethylene elimination from carboxyethylene-bridged bimetallic complexes: Gibson, D. H.; Franco, J. O.; Mehta, J. M.; Harris, M. T.; Ding, Y.; Mashuta, M. S.; Richardson, J. F. *Organometallics* **1995**, *14*, 5078.

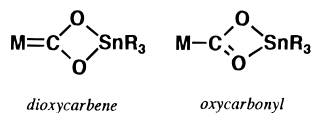
(28) By the oxidation of CO with O₂: John, G. R.; Johnson, B. F. G.; Lewis, J.; Wong, K. C. *J. Organomet. Chem.* **1979**, *169*, C23.

(18) Gibson, D. H.; Ong, T. S.; Ye, M. *Organometallics* **1991**, *10*, 1811.

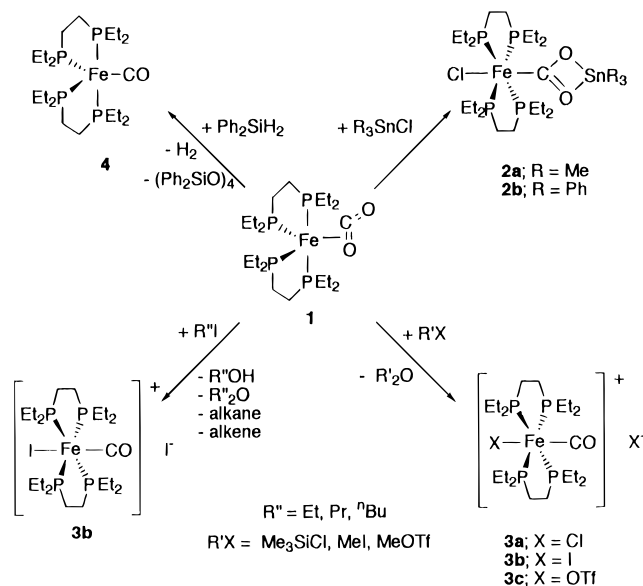
(19) Pinkes, J. R.; Cutler, A. R. *Inorg. Chem.* **1994**, *33*, 759.

(20) Senn, D. R.; Emerson, K.; Larsen, R. D.; Gladysz, J. A. *Inorg. Chem.* **1987**, *26*, 2737.

Chart 2



Scheme 1



carboxylate complexes can be considered. One is the dioxycarbene, and the other is the oxycarbonyl, as illustrated in Chart 2.

It is known that the ¹³C{¹H} NMR spectrum is a useful tool to determine such coordination modes. For example, metal carboxylate complexes having an oxycarbonyl mode such as FeCp(CO₂SnR₃)(CO)L,¹⁸ FeCp*(CO₂SnR₃)(CO)L,¹⁹ and ReCp*(CO₂SnR₃)(CO)(NO)²⁰ (L = CO, PPh₃; R = Me, Ph, ⁿBu) exhibit carboxylate carbon resonances at 197.6–232.0 ppm, while chemical shifts of CO₂ in the dioxycarbene mode such as FeCp(CO₂MCp₂Cl)(CO)₂ (M = Ti, Zr),²³ FeCp[CO₂Re(CO)₃(PPh₃)](CO)(PPh₃),²⁹ and ReCp(CO₂SnPh₃)(CO)(NO)²⁰ appear at 243–275 ppm. Thus, complexes **2a** and **2b** may have some dioxycarbene character in solution because their bridging CO₂ carbons resonate in the intermediate range between oxycarbonyl and dioxycarbene modes. However, the X-ray data apparently exclude the contribution of the carbenoid form in the solid state because two C–O and Sn–O bonds are unequal.

Reaction of 1 with Me₃SiCl, MeI, or MeOTf. Reactions of **1** with other group 14 electrophiles were performed, and the results are outlined in Scheme 1.

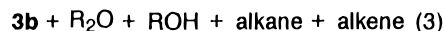
Treatment of **1** with Me₃SiCl in toluene caused a rapid color change from red to yellow, giving (Me₃Si)₂O in 96% yield with respect to Fe and the yellow complex [FeCl(CO)(depe)₂]⁺Cl[−] (**3a**). The latter was purified by recrystallization from MeOH/Et₂O to give yellow crystals. The IR spectrum of **3a** shows a strong ν(C=O) band at 1913 cm^{−1}, suggesting the presence of a carbonyl ligand. The observed frequency is much higher than that in zerovalent Fe(CO)(depe)₂ (1800 cm^{−1}; *vide infra*), reflecting the weaker back-bonding to CO from Fe in **3a**. The high molar electric conductivity of **3a** (11.6 S

Table 3. Product Distribution (%/Fe) in the Reaction of Fe(CO)₂(depe)₂ (**1**) with Carbon Electrophiles

RX	R ₂ O ^a	ROH ^a	alkane ^a	alkene ^a	[FeX(CO)(depe) ₂] ^b X
MeI	81	n.d. ^c	8		97
MeI ^d	2	76	45		89
MeOTf	99	n.d.	n.d.		89
EtI	50	64	12	9	90
PrI	13	23	42	17	78
BuI	1	27	28	11	79

^a The product yield was determined by GLC analysis. ^b Isolated yield. ^c Not detected. ^d 10-fold excess of water with respect to **1** was added.

cm² mol^{−1}) in acetone shows its ionic character. It is especially noteworthy that **1** can react with carbon electrophiles such as MeI and MeOTf to give the analogous cationic carbonyliron(II) complexes [FeI(CO)(depe)₂]⁺I[−] (**3b**) and [Fe(OTf)(CO)(depe)₂]⁺OTf[−] (**3c**) and Me₂O in 81%/Fe and 99%/Fe yields, respectively. While a small amount of methane was observed during the reaction of **1** with MeI (8%/Fe), no methane evolution was observed in the reaction of **1** with MeOTf. The addition of water in the reaction of **1** with MeI dramatically suppressed the formation of Me₂O but enhanced the formation of MeOH and methane. In the reaction of **1** with EtI, PrI, or BuI, the corresponding alkenes in addition to alkanes and alcohols were also generated, accompanied by the formation of **3b** (eq 3 and Table 3).



The C–O bond cleavage of the coordinated CO₂ ligand is not an uncommon process. For example, thermolysis of Nb(Cp*)(CO)₂(CH₂SiMe₃)³⁰ and reactions of [Cp₂TiCl]₂ with CO₂,³¹ and of *trans*-WCl₂(PMePh₂)₄ with CO₂³² gave transition-metal oxo complexes and CO. Exposure of [(np₃)Co(CO)]BPh₄ (np₃ = N(C₂H₄PPh₂)₃) to CO₂ led to disproportionation, giving [(np₃)Co(CO)]BPh₄ and [(np₃O)Co]BPh₄ (np₃O = P(O)Ph₂C₂H₄N(C₂H₄PPh₂)₂).³³ Treatment of Ir₂(CO)₃(μ-CO₂)(dmpm)₂ with CO₂³⁴ and thermolysis of MoCp₂(CO)₂³⁵ afforded transition-metal carbonyl and carbonate complexes. Ir₂[CN(CO)₂R]₂-(CNR)₂(dmpm)₂ reacted with CH₂Cl₂ to give carbonyl and isocyanate ligands in [Ir₂(μ-CO)(μ-H)(C(O)NHR)₂-(CNR)₂(dmpm)₂]⁺Cl[−].³⁶ Treatment of CpRu(CO)(CO₂ZrCp₂Cl) with 2 equiv of the Schwartz reagent gave CpRu(CO)₂(CH₂OZrCp₂Cl) and [Cp₂ZrCl]₂O.³⁷

On the other hand, the reaction of coordinated CO₂ with carbon electrophiles is quite rare to date. For example, although Nicholas et al. reported a similar treatment of Cp₂Mo(CO)₂ with R₃SiCl, giving the cat-

(30) Fu, P.; Khan, M. A.; Nicholas, K. M. *Organometallics* **1991**, *10*, 382.

(31) Fachinetti, G.; Floriani, C.; Chiesi-Villa, A.; Guastini, C. *J. Am. Chem. Soc.* **1979**, *101*, 1767.

(32) Bryan, J. C.; Mayer, J. M. *J. Am. Chem. Soc.* **1990**, *112*, 2298.

(33) Bianchini, C.; Meli, A. *J. Am. Chem. Soc.* **1984**, *106*, 2689.

(34) Reinking, M. K.; Ni, J.; Fanwick, P. E.; Kubiak, C. P. *J. Am. Chem. Soc.* **1989**, *111*, 6459.

(35) Belmore, K. A.; Vanderpool, R. A.; Tsai, J.; Khan, M. A.; Nicholas, K. M. *J. Am. Chem. Soc.* **1988**, *110*, 2004.

(36) Wu, J.; Fanwick, P. E.; Kubiak, C. P. *Organometallics* **1987**, *6*, 1805.

(37) Steffey, B. D.; Vites, J. C.; Cutler, A. R. *Organometallics* **1991**, *10*, 3432.

(38) Tsai, J.-C.; Khan, M.; Nicholas, K. M. *Organometallics* **1989**, *8*, 2967.

(29) Gibson, D. H.; Ye, M.; Richardson, J. F. *J. Am. Chem. Soc.* **1992**, *114*, 9716.

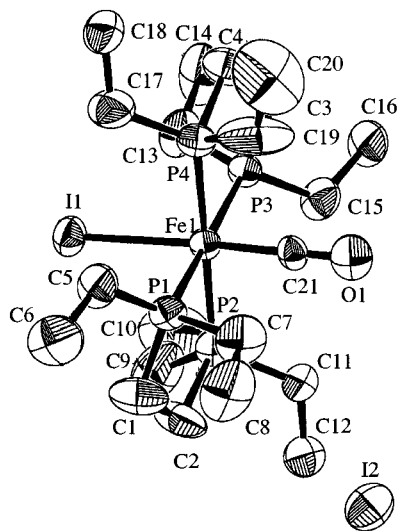


Figure 3. Molecular structure of $[\text{FeI}(\text{CO})(\text{depe})_2]^+\text{I}^-$ (**3b**). Hydrogen atoms are omitted for clarity.

Table 4. Selected Bond Distances (Å) and Angles (deg) in $[\text{FeI}(\text{CO})(\text{depe})_2]^+\text{I}^-$ (**3b**)

Fe(1)–C(21)	1.73(2)	Fe(1)–I(1)	2.696(3)
O(1)–C(21)	1.13(4)	Fe(1)–P(1)	2.288(3)
Fe(1)–P(2)	2.305(3)	Fe(1)–P(3)	2.302(3)
Fe(1)–P(4)	2.308(3)		
I(1)–Fe(1)–C(21)	177.2(4)	O(1)–C(21)–Fe(1)	175(1)
P(1)–Fe(1)–C(21)	92.0(4)	P(2)–Fe(1)–C(21)	89.4(4)
P(3)–Fe(1)–C(21)	86.4(4)	P(4)–Fe(1)–C(21)	90.6(4)

ionic carbonylmolybdenum complex $[\text{Cp}_2\text{MoCl}(\text{CO})]^+\text{Cl}^-$ and $(\text{R}_3\text{Si})_2\text{O}$, and that with $\text{HCo}(\text{CO})_4$, giving $[\text{Cp}_2\text{MoH}(\text{CO})]^+[\text{Co}(\text{CO})_4]^-$ and water, no reaction took place by treatment with MeI .³⁸ On the other hand, Yamamoto et al. recently reported that a zerovalent CO_2 complex of palladium, $\text{Pd}(\text{CO})_2(\text{PMePh}_2)_2$, reacted with Me_3SiCl to give $\text{Me}_3\text{SiSiMe}_3$ and $\text{PdCl}_2(\text{PMePh}_2)_2$ with generation of CO_2 , but the reaction with MeI led to decomposition.¹⁴ However, an iron carboxylate anion, $\text{CpFe}(\text{CO})(\text{PPh}_3)(\text{CO}_2^- \text{K}^+)$, is known to react with MeI , giving $\text{CpFe}(\text{CO})(\text{PPh}_3)(\text{CO}_2\text{Me})$ without C–O bond cleavage.¹⁸ These results suggest that the nucleophilicity of the CO_2 ligand in **1** will be as high as that of the carboxylate complex. Such high reactivity may be due to significant contribution of $\eta^1(\text{C})$ character, which increases the nucleophilicity of the $\eta^2(\text{C}, \text{O})\text{-CO}_2$ ligand.^{39–42}

A single crystal of **3b** suitable for X-ray crystallography was obtained by recrystallization from a mixture of MeOH and Et_2O . The molecular structure of **3b** is depicted in Figure 3, and selected bond distances and angles are listed in Table 4.

Complex **3b** has an octahedral geometry, where the coordinated iodide and the carbonyl ligands are located in a *trans* configuration. The uncoordinated iodide anion was observed as a counteranion far from the metal center. This result is consistent with the ionic character of **3b**. Additionally, the NMR data described above

(39) Tsai, J.; Khan, M. A.; Nicholas, K. M. *Organometallics* **1991**, *10*, 29.

(40) Maher, J. M.; Lee, G. R.; Cooper, N. J. *J. Am. Chem. Soc.* **1987**, *109*, 6797.

(41) Tanaka, H.; Tzeng, B.-C.; Nagao, H.; Peng, S.-M.; Tanaka, K. *Inorg. Chem.* **1993**, *32*, 1508.

(42) (a) Belmore, K. A.; Vanderpool, R. A.; Tsai, J.; Khan, M. A.; Nicholas, K. M. *J. Am. Chem. Soc.* **1988**, *110*, 2004. (b) Tsai, J.; Kahn, M. A.; Nicholas, K. M. *Organometallics* **1989**, *8*, 2967.

show that this structure is retained in solution. It is interesting to note that **3a** and **3b** show a structural preference for the carbonyl carbon and halide ligands to be *trans* to each other. Similarly, the chloride ligand is *trans* to the carboxylate ligand in **2a** and **2b**. Because halide and carbonyl/carboxylate carbon ligands act as good π -donors and π -acceptors, respectively, these structural preferences are best explained for the stabilization by the intramolecular electron transfer from the halide into the carbonyl/carboxylate carbon ligands as a “push–pull” effect.

Similarly, **1** can react with Cp_2TiCl_2 to give the cationic carbonyl complex **3a**.^{43–45} It is interesting to note that the neutral CO_2 ligand in **1** has enough nucleophilicity to react with oxophilic Cp_2TiCl_2 , although the iron carboxylate complex $\text{CpFe}(\text{CO})_2(\text{CO}_2^- \text{Na}^+)$ is known to react with Cp_2TiCl_2 , giving $\text{CpFe}(\text{CO})_2(\text{CO}_2\text{TiCp}_2\text{Cl})$, which immediately degrades to give $[\text{CpFe}(\text{CO})_2]_2$ and $[\text{Cp}_2\text{TiCl}]_2\text{O}$.

Reaction of 1 with Ph_2SiH_2 . Reaction of **1** with Ph_2SiH_2 in toluene at room temperature resulted in the formation of orange solution accompanied by evolution of an almost quantitative amount of hydrogen (92%/Fe). Addition of hexane to the reaction mixture caused preferential precipitation of diphenylsiloxane tetramer $(\text{Ph}_2\text{SiO})_4$ (76%/Fe based on a “ Ph_2SiO ” unit).⁴⁶ From the mother liquor, orange crystals of the zerovalent iron carbonyl complex $\text{Fe}(\text{CO})(\text{depe})_2$ (**4**) were isolated in 57% yield. It is worthwhile to note that a direct reduction of the coordinated CO_2 takes place without a change in the formal oxidation state of the metal center. The low molar electric conductivity ($\Lambda = 0.0183 \text{ S cm}^2 \text{ mol}^{-1}$) indicates the nonionic character of **4**. Complex **4** can also be prepared by the reaction of $\text{Fe}(\text{N}_2)(\text{depe})_2$ with CO , as reported previously.⁴⁷

Mechanism of the Reaction of 1 with Group 14 Electrophiles. Formation of the iron carboxylate **2** and the cationic carbonyl complex **3** can be interpreted by the mechanism shown in Scheme 2.

First of all, an electrophile (RX) such as MeI , Me_3SiCl , Me_3SnCl , or Ph_3SnCl directly interacts with one of the oxygen atoms of the CO_2 ligand to give metal carboxylate **A**. In the reactions with organotin chlo-

(43) The fate of the titanium fragment is unclear to date. This reaction gave a single sole titanium product, because a singlet peak at δ 6.6 assignable to a sole Cp resonance was observed by ^1H NMR spectrum in C_6D_6 . Dechlorination from Cp_2TiCl_2 and deoxygenation from **1** took place simultaneously in this reaction. Therefore, we expected that the most probable titanium product would be $[\text{Cp}_2\text{TiCl}]_2\text{O}$,⁴⁴ by taking into account the reaction pattern of other electrophiles. However, other titanium complexes such as $[\text{Cp}_2\text{TiO}]_n$ ⁴⁵ could not be ruled out. Unfortunately, further purification of the titanium fragment failed and thus left its fate inconclusive.

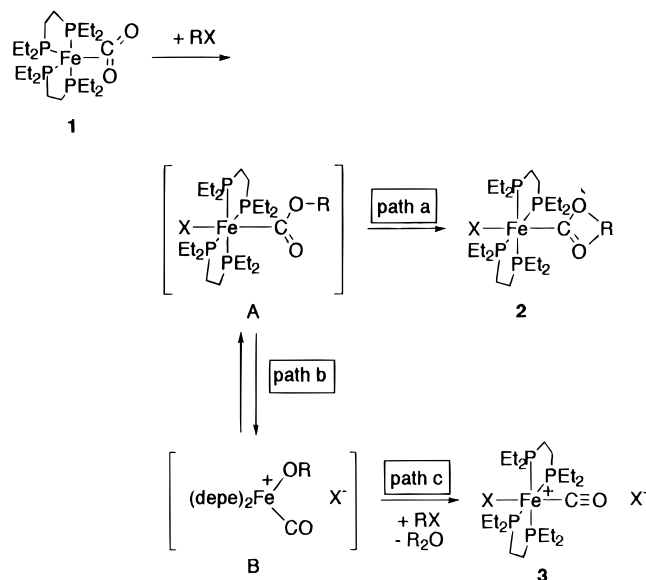
(44) (a) Giddings, S. A. *Inorg. Chem.* **1964**, *3*, 684. (b) Bottomley, F.; Lin, I. J.; Mukaida, M. *J. Am. Chem. Soc.* **1980**, *102*, 5238. (c) Fachinetti, G.; Floriani, C.; Chiesi-Villa, A.; Guastini, C. *J. Am. Chem. Soc.* **1979**, *101*, 1767.

(45) Cp_2TiO would be also a possible product. However, it may polymerize with the composition $[\text{Cp}_2\text{TiO}]_n$, which is difficult to isolate under these conditions. Only one example of the isolation of a titanocene oxide analogue has been reported in the presence of Lewis bases; Smith, M. R., III; Matsunaga, P. T.; Andersen, R. A. *J. Am. Chem. Soc.* **1993**, *115*, 7049.

(46) Diphenylsiloxane tetramer was characterized by ^1H NMR, IR, and GC–MS spectra and elementary analysis in comparison with authentic material prepared by the following literature method: Takiguchi, T. *J. Org. Chem.* **1959**, *24*, 989.

(47) After our communication dealing with this reaction had been published,¹² Jones et al. also detected the formation of $\text{Fe}(\text{CO})(\text{depe})_2$ from the treatment of $\text{Fe}(\text{N}_2)(\text{depe})_2$ with CO : Perthuisot, C.; Jones, W. D. *New J. Chem.* **1994**, *18*, 621. The X-ray structure analysis will be reported separately. Hirano, M.; Akita, M.; Morikita, T.; Kubo, H.; Fukuoka, A.; Komiya, S. *J. Chem. Soc., Dalton Trans.*, in press.

Scheme 2



rides, stable heterodinuclear iron carboxylates **2** were isolated (path a). When stronger electrophiles were employed, decarboxylation took place to give alkoxycarbonyliron(II) halides B (path b). Intermediates A and B further react with another electrophile (RX) to form the corresponding ethers (R₂O) and halogenocarbonyliron(II) halides **3** (path c). The fate of the CO₂ ligand may depend on the Lewis acidity of the electrophile used, because weak Lewis acids such as organotin chlorides afforded the iron carboxylate, while the other stronger Lewis acids such as MeI, Me₃SiCl, and Cp₂-TiCl₂ led to C–O bond cleavage. It is interesting to note that strong Brønsted acids also enhance C–O bond cleavage in the electrochemical reduction of CO₂ by use of iron(0) porphyrin.⁴⁸

In the presence of a trace amount of water, parts of these complexes were hydrolyzed to liberate the corresponding alcohol. In the reactions with alkyl iodides a small amount of alkane was always formed, suggesting the formation of an alkyliron species in the reaction. The presence of water in the reaction mixture enhanced the formation of the alkane and alcohol as shown in Table 3, supporting this assumption. Formation of alkene in the reaction of ethyl, propyl, and butyl iodides may arise from β-hydrogen elimination out of possible alkyliron intermediates. Accordingly, if a highly reactive electrophile such as MeOTf was used, formation of alkane was suppressed and quantitative formation of Me₂O was observed.

In the reaction of **1** with dihydrosilane Ph₂SiH₂, quantitative formation of hydrogen and (Ph₂SiO)₄ was observed and the resulting iron complex was the zerovalent Fe(CO)(depe)₂. The mechanism of the reaction is not clear at present, though diphenylsiloxane tetramer may be formed by cyclooligomerization of the diphenylsiloxo moiety which is produced by β-hydrogen elimination from a (hydrodiphenylsiloxo)iron(II) intermediate accompanied by the reduction of iron metal.

Experimental Section

General Procedures. All manipulations were performed under dry nitrogen using standard Schlenk and vacuum-line

techniques. All solvents were distilled from appropriate drying agents prior to use. Carbon dioxide was deoxygenated and dried by the freeze–pump–thaw method prior to use. Fe(N₂)(depe)₂ was synthesized according to the method published in our previous paper.¹² ¹H and ¹³C{¹H} NMR spectra were recorded on JEOL FX-200 or LA-300 spectrometers, and chemical shifts are reported in ppm from internal TMS. ³¹P{¹H} NMR spectra were recorded on JEOL LA-300 or Bruker AM-400 spectrometers, and chemical shifts are reported in ppm downfield from external 85% H₃PO₄ or PPh₃. IR spectra were recorded on a JASCO FT/IR-5M spectrometer. Mass spectra were recorded on a Shimadzu GC-MS QP-2000 spectrometer. GLC analyses of gases were performed with a Shimadzu GC-3BT gas liquid phase chromatograph using stainless steel columns packed with molecular sieves or active carbon with TCD detector. The volume of generated gases was measured by a Toepler pump. Melting points were measured under nitrogen with a Yazawa MP-21 capillary melting apparatus, and the values are uncorrected. Elemental analyses were performed with a Yanaco CHN MT-2 autocorder or a Perkin-Elmer 2400 series II CHN analyzer. Molar electric conductivities were measured by a TOA Model CM-7B instrument.

Fe(CO)₂(depe)₂ (1). A stoichiometric amount of CO₂ (2.27 mL, 1.01 mmol) was introduced into a THF (40 mL) solution of Fe(N₂)(depe)₂ (503.7 mg, 1.01 mmol) at room temperature under reduced pressure. After 1 h of stirring, N₂ was detected (87%/Fe). A red solid was obtained after removal of the solvent under reduced pressure. Recrystallization of the red solid from Et₂O gave red prisms of **1** (356.6 mg, 70%/Fe). Mp: 94–96 °C dec. Molar electric conductivity in acetone: Λ = 0.0168 S cm² mol⁻¹ (25 °C). M_w (cryoscopic method): 501 (calcd for C₂₁H₄₈FeO₂P₄ 512). ¹H NMR (200 MHz, C₆D₆): δ 0.5–1.5 (m). ³¹P{¹H} NMR (162 MHz, C₆D₆, external PPh₃): δ 68.13 (dt, J = 17, 29 Hz), 82.44 (ddd, J = 29, 42, 127 Hz), 84.44 (ddd, J = 17, 49, 127 Hz), 92.44 (ddd, J = 29, 42, 49 Hz). ¹³C{¹H} NMR (100 MHz, C₆D₆): 196.6 (qui, J = 38 Hz). IR (KBr, cm⁻¹): 1630 (ν_{CO}), 1096 (ν_{CO}), 732 (δ_{OCO}). Anal. Calcd for C₂₁H₄₈FeO₂P₄: C, 49.11; H, 10.17. Found: C, 49.23; H, 10.90.

FeCl(CO₂SnR₃)(depe)₂ (2). To an Et₂O solution (10 mL) of **1** (172.1 mg, 0.336 mmol) was added an Et₂O solution (8 mL) of Me₃SnCl (69.1 mg, 0.346 mmol) by cannula tube at –78 °C. The reaction mixture was stirred for 2 h, during which time the temperature was raised to room temperature. The color of the solution gradually changed from red to orange. After removal of a small amount of insoluble materials, the resulting deep orange solution was concentrated to about one-third of the original volume and kept at –30 °C to yield red cubes of FeCl(CO₂SnMe₃)(depe)₂ (**2a**; 108.7 mg, 46%/Fe). Mp: 88–90 °C dec. Molar electric conductivity in acetone: Λ = 9.7 S cm² mol⁻¹ (25 °C). ¹H NMR (300 MHz, C₆D₆): δ 0.22 (s, J = 71 Hz, SnMe₃, 9H), 1.1–2.6 (m, depe). ³¹P{¹H} NMR (121.6 MHz, C₆D₆, 85% H₃PO₄ in D₂O as external standard): δ 71.6 (s). ¹³C{¹H} NMR (100 MHz, C₆D₆): δ –2.0 (s, J_{Sn-C} = 189 Hz), 9.7 (s), 10.1 (s), 17.5 (s), 20.2 (qui, J_{C-P} = 10 Hz), 21.6 (s), 239.5 (qui, J_{C-P} = 24 Hz). IR (KBr): 1338 (w, ν_{CO}) cm⁻¹. Anal. Calcd for C₂₄H₅₇ClFeO₂P₄Sn: C, 40.51; H, 8.07. Found: C, 40.95; H, 7.86. A similar treatment of **1** (161.0 mg, 0.314 mmol) with Ph₃SnCl (122.2 mg, 0.317 mmol) resulted in the formation of FeCl(CO₂SnPh₃)(depe)₂ (**2b**). Recrystallization from cold Et₂O gave orange cubes of **2b** (124.8 mg, 0.139 mmol, 44%/Fe). Mp 119.5–121.5 °C (dec). Molar electric conductivity in acetone: Λ = 0.41 S cm² mol⁻¹ (25 °C). ¹H NMR (300 MHz, C₆D₆): δ 0.98 (br, depe, 12H), 1.06 (br, depe, 12H), 1.45 (sext, J = 7 Hz, depe, 4H), 1.55 (sext, J = 7 Hz, depe, 4H), 1.74 (br, depe, 4H), 2.02 (m, depe, 8H), 2.48 (sext, J = 7 Hz, depe, 4H), 7.1–7.3 (m, SnPh₃, 9H), 7.78 (d, J = 7 Hz, *ortho* protons of SnPh₃, 6H). ³¹P{¹H} NMR (121.6 MHz, C₆D₆, 85% H₃PO₄ in D₂O as external standard): δ 74.7 (s). ¹³C{¹H} NMR (75.45 MHz, C₆D₆): δ 9.7 (s), 10.0 (s), 18.8 (br), 20.4 (qui, J_{C-P} = 11 Hz), 21.4 (m), 128.8 (almost overlapped with a signal of C₆D₆), 137.5 (d, J_{Sn-C} = 22 Hz), 144.2 (d, J_{Sn-C} = 308 Hz), 243.8 (qui,

(48) Bhugun, I.; Lexa, D.; Savéant, J.-M. *J. Am. Chem. Soc.* **1996**, *118*, 1769.

$J_{C-P} = 22$ Hz). IR (KBr): 1306 (w, ν_{CO}) cm^{-1} . Anal. Calcd for $C_{39}H_{63}ClFeO_2P_4Sn$: C, 52.29; H, 7.09. Found: C, 51.96; H, 7.12.

Reaction of 1 with Me_3SiCl . A toluene (1 mL) solution of **1** (81.7 mg, 0.159 mmol) was degassed by three freeze–pump–thaw cycles. Me_3SiCl (40 μL , 0.32 mmol) was added by the hypodermic syringe, during which the red solution immediately changed to a yellow suspension. The resulting mixture was allowed to react for 2 h at room temperature. No gas evolution was observed by the Toepler pump. In solution (Me_3Si)₂O was detected (0.152 mmol, 96%/Fe) by GLC analysis. Then, all the volatile materials were removed under reduced pressure, and the resulting yellow solid was recrystallized from a mixture of MeOH/Et₂O to give $[FeCl(CO)(depe)_2]^+Cl^-$ (**3a**; 76.3 mg, 0.135 mmol, 84%/Fe). Mp 241–242 °C dec. Molar electric conductivity in acetone: $\Lambda = 11.6$ S $\text{cm}^2 \text{mol}^{-1}$ (25 °C). ¹H NMR (200 MHz, C₆D₆): δ 1.32–2.48 (br, depe). IR (KBr): 1913 (ν_{CO}), 1460, 1416, 1378 (depe) cm^{-1} . Anal. Calcd for $C_{21}H_{48}Cl_2FeOP_4$: C, 44.46; H, 8.52; Cl, 12.5. Found: C, 43.90; H, 8.74; Cl, 13.2.

Reaction of 1 with MeI. A toluene (1 mL) solution of **1** (51.5 mg, 0.101 mmol) was degassed by three freeze–pump–thaw cycles. MeI (310 μL , 4.98 mmol) was added by hypodermic syringe. The reaction mixture was stirred at room temperature under vacuum for 13 h, during which time the red solution changed to a light yellow suspension. Methane (0.18 mL, 0.0082 mmol, 8%/Fe) and Me₂O (2.0 mL, 0.088 mmol, 87%/Fe) were generated during the reaction. Addition of hexane (3 mL) resulted in the formation of a yellow precipitate. Recrystallization of the resulting precipitate gave $[FeI(CO)(depe)_2]^+I^-$ (**3b**; 73.3 mg, 0.0977 mmol, 97%/Fe). Mp: 242–244 °C dec. Molar electric conductivity in acetone: $\Lambda = 31.5$ S $\text{cm}^2 \text{mol}^{-1}$ (25 °C). ¹H NMR (200 MHz, C₆D₆): δ 1.19–2.72 (br, depe). IR (KBr): 1937 (ν_{CO}), 1458, 1411, 1377 (depe) cm^{-1} . Anal. Calcd for $C_{21}H_{48}FeI_2OP_4$: C, 33.62; H, 6.45; I, 33.83. Found: C, 33.52; H, 6.70; I, 34.03.

Reaction of 1 with MeI in the Presence of Water. An ethylbenzene (1 mL) solution of **1** (34.5 mg, 0.0673 mmol) was degassed by three freeze–pump–thaw cycles. H₂O (12 μL , 0.66 mmol) and then MeI (210 μL , 3.37 mmol) were added by hypodermic syringe. After 13 h of reaction at room temperature under vacuum, methane (0.68 mL, 0.03 mmol, 45%/Fe), MeOH (0.051 mmol, 76%/Fe), and Me₂O (0.0014 mmol, 2%/Fe) were observed. All volatiles were removed in vacuo. Recrystallization of the resulting solid from a mixture of methanol/ether gave **3b** (44.9 mg, 89%/Fe).

Reaction of 1 with MeOTf. A toluene (1 mL) solution of **1** (76.4 mg, 0.149 mmol) was degassed by three freeze–pump–thaw cycles. MeOTf (170 μL , 1.50 mmol) was added by hypodermic syringe. The reaction mixture was stirred at room temperature under vacuum for 3 h. Neither methane nor methanol was detected, but Me₂O (0.147 mmol, 98.6%/Fe) was formed after the reaction. After removal of all volatile materials, $[Fe(OTf)(CO)(depe)_2]^+OTf^-$ (**3c**; 44.9 mg, 88.9%/Fe) was obtained from recrystallization of the residual solid from MeOH/Et₂O. Mp: 148–151 °C dec. Molar electric conductivity in acetone: $\Lambda = 15.7$ S $\text{cm}^2 \text{mol}^{-1}$ (25 °C). ¹H NMR (200 MHz, C₆D₆): δ 1.15–2.51 (br, depe). IR (KBr, cm^{-1}): 1938 (ν_{CO}). Anal. Calcd for $C_{23}H_{48}F_6FeO_7P_4S_2$: C, 34.77; H, 6.06. Found: C, 34.10; H, 6.62.

Reaction of 1 with EtI. A THF (1 mL) solution of **1** (58.4 mg, 0.114 mmol) was degassed by three freeze–pump–thaw cycles. EtI (460 μL , 5.75 mmol) was added by hypodermic syringe. The reaction mixture was stirred at room temperature for 15 h. Ethane (0.19 mL, 0.0084 mmol, 7.3%/Fe), ethylene (0.239 mL, 0.011 mmol, 9.4%/Fe), EtOH (0.051 mmol, 45%/Fe), and Et₂O (0.039 mmol, 35%/Fe) were formed during the reaction. After removal of volatile materials, recrystallization from MeOH/Et₂O gave **3b** (75.9 mg, 88.7%/Fe).

Reaction of 1 with PrI. An ethylbenzene (1 mL) solution of **1** (39.1 mg, 0.0763 mmol) was degassed by three freeze–pump–thaw cycles. PrI (420 μL , 3.82 mmol) was added by

hypodermic syringe. The reaction mixture was stirred at room temperature for 12 h, during which time the red solution gradually changed to a light yellow suspension. Propane (0.71 mL, 0.032 mmol, 42%/Fe), propylene (0.28 mL, 0.013 mmol, 13%/Fe), PrOH (0.018 mmol, 42%/Fe), and Pr₂O (0.010 mmol, 13%/Fe) were formed during the reaction. After removal of volatile materials, recrystallization from MeOH/Et₂O gave **3b** (44.7 mg, 78%/Fe).

Reaction of 1 with BuI. An ethylbenzene (1 mL) solution of **1** (35.9 mg, 0.0700 mmol) was degassed by three freeze–pump–thaw cycles. BuI (400 μL , 3.51 mmol) was added by hypodermic syringe. The reaction mixture was stirred at room temperature for 12 h, during which time the red solution gradually changed to a light yellow suspension. Butane (0.17 mL, 0.0076 mmol, 28%/Fe), 1-butene (0.17 mL, 0.076 mmol, 28%/Fe), BuOH (0.019 mmol, 27%/Fe), and Bu₂O (0.0010 mmol, 1%/Fe) were formed during the reaction. After addition of hexane (3 mL), the resulting precipitate was recrystallized from MeOH/Et₂O to give **3b** (41.3 mg, 79%/Fe).

Reaction of 1 with Ph₂SiH₂. A toluene (1 mL) solution of **1** (99.2 mg, 0.194 mmol) with Ph₂SiH₂ (43.0 μL , 0.232 mmol) was reacted for 12 h at room temperature, during which time the solution color changed from red to orange. An almost quantitative amount of hydrogen (0.178 mmol, 92%/Fe) was observed by Toepler pump and GLC analysis. To the orange solution was added dry hexane (2 mL) to give white crystals of (Ph₂SiO)₄ (29.2 mg, 0.368 mmol, 76%/Fe). After filtration of the mother liquor followed by concentration to dryness and recrystallization from pentane, orange crystals of **4** were obtained (54.7 mg, 0.110 mmol, 57%/Fe). Mp: 198–201 °C dec. Molar electric conductivity in acetone: $\Lambda = 0.0183$ S $\text{cm}^2 \text{mol}^{-1}$ (25 °C). ¹H NMR (200 MHz, C₆D₆): δ 0.88–1.93 (m, depe). ³¹P{¹H} NMR (162 MHz, C₇D₈, PPh₃ as an external standard): δ 91.59 (s, 25 °C), 96.77 (s, –55 °C). IR (KBr): 1800 (s, ν_{CO}) cm^{-1} . Anal. Calcd for $C_{21}H_{48}FeOP_4$: C, 50.82; H, 9.75. Found: C, 51.39; H, 9.99.

Reaction of 1 with Cp₂TiCl₂. A benzene solution (8 mL) of **1** (86.3 mg, 0.168 mmol) and Cp₂TiCl₂ (37.9 mg, 0.152 mmol) was stirred at room temperature under vacuum for a night. The reaction mixture changed from a deep red solution to a light green suspension. No noncondensable gases at –78 °C were detected by Toepler pump. The precipitate was collected and characterized as **3a** (77.1 mg, 81%/Fe). The fate of the Ti compound is unclear to date, however. ¹H NMR (200 MHz, C₆D₆): δ 6.6 (s, Cp).

Crystallographic Analyses. All crystals were mounted in glass capillaries (GLAS, 0.7 mm i.d.) under an argon atmosphere. The data were collected at 23 °C using the TEXSAN automatic data collection series on a Rigaku AFC5R diffractometer using Mo K α radiation ($\lambda = 0.71069$ Å). Absorption correction was not performed for any of the complexes. The crystallographic data for **2b** and **3b** are summarized in Table 5.

X-ray Analysis of Fe(CO)₂(depe)₂ (1). A suitable crystal was obtained from a saturated Et₂O solution of **1**. One of the selected crystals was mounted on a glass capillary. No crystal decay was noticed during the data collection. Crystal data: $C_{21}H_{48}FeO_2P_4$, $f_w = 512.35$; monoclinic, Cc , $a = 12.681(1)$ Å, $b = 15.948(2)$ Å, $c = 13.354(3)$ Å, $\beta = 90.75(1)^\circ$; $V = 2700.5(6)$ Å³, $Z = 4$, $D_{\text{calcd}} = 1.260$ g cm^{-3} , $\mu(\text{Mo K}\alpha) = 8.09$ cm^{-1} . Using the criterion $|F_o| > 3.0\sigma(|F_o|)$, where $\sigma(|F_o|)$ is the estimated standard deviation derived from the counting statistics, 1191 out of the 2035 reflections were used for calculation. The structure was solved by heavy-atom methods. Full details, including tables of bond distances and angles, thermal parameters, and F_o/F_c values, are available as Supporting Information to ref 11 or by application to the Cambridge Crystallographic Data Centre.

X-ray Analysis of FeCl(CO₂SnPh₃)(depe)₂ (2b). Clear and reddish orange crystals were grown from a saturated solution of **2b** in Et₂O. A crystal of suitable size was selected and mounted in a glass capillary tube. Crystal and instrument

Table 5. Crystal Data and Structure Refinement Parameters for 2b and 3b

	2b	3b
formula	C ₃₉ H ₆₃ ClFeO ₂ P ₄ Sn	C ₂₁ H ₁₈ FeI ₂ OP ₄
fw	897.81	750.16
cryst syst	monoclinic	monoclinic
space group	<i>P2</i> ₁	<i>P2</i> ₁ / <i>a</i>
unit cell dimens		
<i>a</i> (Å)	10.121(4)	20.538(4)
<i>b</i> (Å)	15.056(5)	14.45(3)
<i>c</i> (Å)	14.636(3)	10.234(2)
β (deg)	103.74(2)	99.99(1)
<i>V</i> (Å ³)	2166(1)	2991(3)
<i>Z</i>	2	4
<i>D</i> _{calcd} (g cm ⁻³)	1.376	1.665
μ(Mo Kα) (mm ⁻¹)	1.151	2.794
temp (°C)	23	23
2θ range (deg)	3.0 < 2θ < 55.0	6.0 < 2θ < 45.0
no. of data collected	5474	4356
no. of obsd rflns for refinement	3448 ($ F_o > 3\sigma F_o $)	2801 ($ F_o > 3\sigma F_o $)
<i>R</i> ^a	0.052	0.052
<i>R</i> _w ^b	0.030	0.060
<i>S</i>	2.54	1.71
method of phase determ	heavy-atom method	direct methods

$$^a R = \sum(|F_o| - |F_c|)/\sum|F_o|. \quad ^b R_w = [\sum w(|F_o| - |F_c|)^2/\sum w|F_o|^2]^{0.5}.$$

stabilities were checked by measuring 3 standard reflections after every 200 observations. No crystal decay was noticed during the data collection. The crystal system was monoclinic, and the space group was *P2*₁. Selected bond distances and angles are listed in Table 2. The unique set contained 5474 reflections within 3.0 < 2θ < 55.0°. Using the criterion $|F_o| > 3.0\sigma(|F_o|)$, 3448 out of the 5474 reflections were used. The structure was solved by heavy-atom methods. High thermal displacement motion was cited for the C(8), C(10)–C(12), and C(20) atoms, suggesting some degree of disorder, but no resolvable disorder could be found. Thus, these atoms were refined isotropically and the other non-hydrogen atoms were refined anisotropically. The hydrogens were located on ideal positions and were refined isotropically. The final *R* (*R*_w) value was 0.052 (0.030). Similarly, crystals of FeCl(CO)₂SnMe₃(depe)₂ (**2a**) were grown from a cold Et₂O solution. However, over the course of data collection, the standards decreased by

–27.3% and the molecular structure was therefore insufficiently solved. The preliminary results suggested that no significant difference between the overall structures of **2a** and **2b** was observed. The crystallographic data of **2a** will be reported elsewhere.

X-ray Analysis of [FeI(CO)(depe)₂]⁺I⁻ (3b**).** A suitable crystal was obtained from a saturated MeOH/Et₂O solution of **3b**. Crystal and instrument stabilities were checked by measuring 3 standard reflections after every 150 observations. The crystal system was monoclinic, and the space group was *P2*₁/*a*. The unique set contained 4356 reflections. Using the criterion $|F_o| > 3.0\sigma(|F_o|)$, 2801 out of the 4356 reflections were used. The structure was solved by direct methods. All non-hydrogen atoms were refined anisotropically. All hydrogen atoms were located on the ideal positions and were refined isotropically. The unit cell showed a 95:5 disorder of the coordinated iodide and carbonyl group (I(1) with I(3), C(21) with C(22), and O(1) with O(2)). The I(3) was found from the difference Fourier map, and the population was determined from the results of the least-squares refinements. On the other hand, because the corresponding disordered carbonyl group C(22) and O(2) could not be found from the difference Fourier map, they were located on calculated positions by a point symmetry of the major CO group at Fe with estimated population for I(3). I(3), C(22), and O(2) were fixed on calculated positions during the refinements. The final *R* (*R*_w) value was 0.052 (0.060).

Acknowledgment. We are grateful to Prof. A. Miyashita of Saitama University for measurement of the low-temperature ³¹P{¹H} NMR spectrum of **4**. This work was financially supported by a Grant-in-Aid for Scientific Research from the Ministry of Education, Science, Sports, and Culture, Japan.

Supporting Information Available: Tables of crystal data and data collection details, fractional coordinates, anisotropic thermal parameters, and bond distances and angles for **2b** and **3b** (22 pages). Ordering information is given on any current masthead page.

OM960743M